RESEARCH ARTICLE • OPEN ACCESS

Mathematical Modeling on Human Papillomavirus (HPV): Transmission Dynamics and Impact on Cervical Cancer

Sayooj Aby Jose *et al.*

Volume 6, Issue 4, Pages 376–385, December 2025

Received 6 January 2025, Revised 21 March 2025, Accepted 17 December 2025, Published Online 31 December 2025

To Cite this Article : S. A. Jose *et al.*,"Mathematical Modeling on Human Papillomavirus (HPV): Transmission Dynamics and Impact on Cervical Cancer", *Jambura J. Biomath*, vol. 6, no. 4, pp. 376–385, 2025, *https://doi.org/10.37905/jjbm.v6i4.29641*

JOURNAL INFO • JAMBURA JOURNAL OF BIOMATHEMATICS

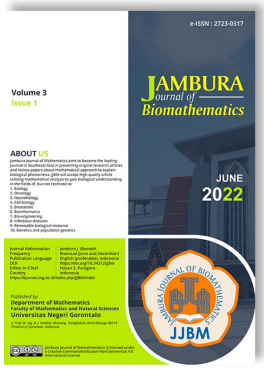

Homepage	:	http://ejurnal.ung.ac.id/index.php/JJBM/index
Journal Abbreviation	:	Jambura J. Biomath.
Frequency	:	Quarterly (March, June, September and December)
Publication Language	:	English
DOI	:	https://doi.org/10.37905/jjbm
Online ISSN	:	2723-0317
Editor-in-Chief	:	Hasan S. Panigoro
Publisher	:	Department of Mathematics, Universitas Negeri Gorontalo
Country	:	Indonesia
OAI Address	:	http://ejurnal.ung.ac.id/index.php/jjbm/oai
Google Scholar ID	:	XzYgeKQAAAAJ
Email	:	editorial.jjbm@ung.ac.id

JAMBURA JOURNAL • FIND OUR OTHER JOURNALS

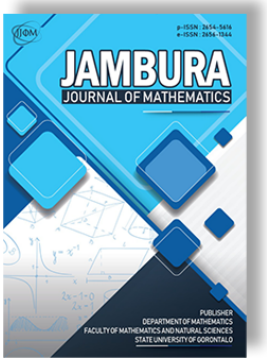

Jambura Journal of Mathematics

Jambura Journal of Mathematics Education

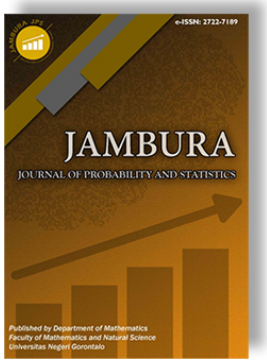

Jambura Journal of Probability and Statistics

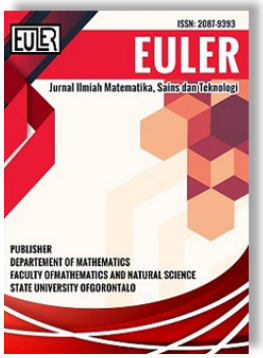

EULER : Jurnal Ilmiah Matematika, Sains, dan Teknologi

Jambura Journal of Biomathematics, Volume 6, Issue 4, Pages 376–385, December 2025 https://doi.org/10.37905/jjbm.v6i4.29641

Research Article

Check for updates

Mathematical Modeling on Human Papillomavirus (HPV): Transmission Dynamics and Impact on Cervical Cancer

Sayooj Aby Jose[1,2], **Stephen Patrick Nelson**[3], **Ramachandran Raja**[3,4], **Gayathry Radhakrishnan Menon**[2], **and Anuwat Jirawattanapanit**[1,*]

[1]*Department of Mathematics, Faculty of Education, Phuket Rajabhat University, Phuket, Thailand*
[2]*School of Mathematics and Statistics , Mahatma Gandhi University, Kottayam, India*
[3]*Ramanujan centre for Higher Mathematics, Alagappa University, Karaikudi-630 004, India*
[4]*Department of Computer Science and Mathematics, Lebanese American University, Beirut, Lebanon*

ARTICLE HISTORY
Received 6 January 2025
Revised 21 March 2025
Accepted 17 December 2025
Published 31 December 2025

KEYWORDS
Mathematical modeling
Cervical Cancer
Reproduction Number
Stability

ABSTRACT. *One of the most common diseases affecting women globally is cervical cancer, which contributes significantly to the global cancer burden. Its beginning is largely caused by the human papillomavirus (HPV), especially in young females, and a growing percentage of cases develop from benign tumors. The dynamics of HPV transmission and its influence on the development of cervical cancer are described in this study using a deterministic mathematical model. The fundamental characteristics of the model, such as positivity and boundedness, are carefully examined. Furthermore, the equilibrium points for endemic and disease-free conditions are determined, and their stability on a local and global scale is examined in relation to the basic reproduction number, R_0. Furthermore, a detailed sensitivity analysis is conducted to identify the key parameters that most significantly influence the transmission dynamics and progression of the disease. Numerical simulations are performed to illustrate the impact of parameter variations and to validate the analytical findings. The results provide valuable insights for effective public health intervention and control strategies for HPV-related cervical cancer.*

1. Introduction

Mathematical modeling is a key tool utilized across various fields to examine complex structures and forecast their dynamics. These models are utilized across various domains, extending beyond engineering disciplines such as electrical engineering and computer science to encompass a wide range of fields including psychology, economics, political science, sociology, as well as the natural sciences like physics, biology, earth science, and chemistry [1–5]. Mathematical modeling has been essential in the study of epidemiology for numerous decades. By offering a quantitative framework, these models allow for the examination of transmission dynamics of infectious diseases, prediction of their potential spread, and assessment of the effectiveness of public health intervention strategies [6, 7].

An important application of mathematical modeling in the field of epidemiology involves examining the transmission of Human Papillomavirus (HPV) and its connection to the beginning of cervical cancer. Cervical cancer continues to be a significant global public health concern, with around 604,000 new cases and 342,000 deaths stated in 2020, predominantly affecting low- and middle-income nations [8]. By employing mathematical models, one can gain deeper insights into the transmission patterns of HPV, evaluate vaccination and screening initiatives, and formulate optimal control strategies designed to decrease the incidence and mortality linked to cervical cancer.

The primary driver of this cancer is the persistent infection with high-risk types of Human Papillomavirus (HPV), particularly types 16 and 18, which are responsible for about 70% of cervical cancer cases [8]. Factors contributing to the high rates of cervical cancer include limited access to vaccination, inadequate screening programs, and socioeconomic disparities that hinder preventive care. Furthermore, co-infection with HIV increases susceptibility to HPV-related cervical lesions, exacerbating the incidence of cervical cancer among affected populations [8]. Cervical cancer poses significant risks to women's health, with lifestyle factors and socioeconomic conditions playing critical roles in its incidence. Factors such as early onset of sexual activity, multiple sexual partners, and inconsistent use of barrier contraception can increase the likelihood of Human Papillomavirus (HPV) infection, the primary cause of cervical cancer. Additionally, smoking has been associated with a twofold increase in the risk of developing cervical cancer, as tobacco by-products can damage cervical cells and impair the immune response against HPV [9, 10]. Women in low-income regions often lack access to preventive healthcare services, including regular screenings and vaccinations, which are crucial for early detection and prevention of HPV-related lesions [10]. Cultural factors may also discourage women from seeking medical care, leading to late-stage diagnoses and poorer health outcomes, Furthermore the availability of HPV vaccines is not uniform across different geographic regions, resulting in unequal

*Corresponding Author.

Email : *anuwat.j@pkru.ac.th* (A. Jirawattanapanit)
Homepage : http://ejurnal.ung.ac.id/index.php/JJBM/index / E-ISSN : 2723-0317

protection against cervical cancer. Addressing these multifaceted risk factors is essential to improve women's health globally and implement effective public health strategies tailored to specific populations [9, 10]. The most prevalent genital tract cancer in women, second only breast cancer, is cervicoma. It affects young women between the ages of 35 and 50. More than 200 different types of viruses make up the HPV family, of which 40 are transmitted through sexual activity [11–13]. The main causes of cervical cancer worldwide are genital HPVs, which are sexually transmitted [14]. Two groups of sexually transmitted HPV types exist: low-risk genotypes, which are those that only produce warts, and high-risk genotypes, which can result in a variety of cancers in females, including cervical cancer [12, 15, 16]. The importance of control strategies including prevention, vaccination, and treatment in particular areas has been highlighted by several HPV and transmission dynamics of cervical cancer models [17, 18]. Looking ahead to 2030, projections indicate that the burden of cervical cancer may continue to rise if current trends and inequities in healthcare access persist. Without significant increases in vaccination rates and screening programs, the incidence of cervical cancer is expected to increase, particularly in low-resource settings where disparities in healthcare are pronounced. Recent data suggests that as many as 60% of women in low-income countries remain unvaccinated against HPV, putting them at a higher risk of developing cervical cancer later in life [19]. Additionally, the social determinants of health, such as education and economic status, will likely exacerbate these risks, leading to a higher prevalence of cervical lesions and late-stage diagnoses. The continued neglect of preventive measures and education about HPV could lead to a stubborn rise in cervical cancer cases, emphasizing the urgent need for targeted public health interventions to mitigate this looming health crisis [20]. To effectively overcome the risks associated with cervical cancer, a multifaceted approach involving vaccination, regular screening, and public education is essential.The introduction of the HPV vaccine is one of the most significant preventive measures; studies indicate that comprehensive vaccination programs can reduce the incidence of cervical cancer by up to 90% when implemented before the onset of sexual activity, particularly among preteens and adolescents. Regular cervical cancer screenings, such as Pap tests and HPV testing, are critical for early detection of precancerous changes, allowing for timely intervention [10]. These screenings should begin at age 21 and be conducted at regular intervals as recommended by healthcare professionals. Public education campaigns are also vital to increase awareness about the importance of HPV vaccination, safe sexual practices, and the need for routine screenings [21]. Also, improving healthcare access in underserved populations through community outreach programs can significantly enhance prevention efforts and reduce disparities in cervical cancer incidence. By implementing these strategies collectively, the overall risk of cervical cancer can be significantly mitigated.

The primary focus of this study is to develop a comprehensive mathematical model describing the transmission dynamics of HPV and to analyze its behavior. Specifically, the model is constructed and its stability is investigated with respect to the disease-free equilibrium point (DFEP). A sensitivity analysis of the model parameters is then performed to identify which factors most significantly influence disease transmission, alongside the calculation of the basic reproduction number, R_0 to quantify the potential for HPV to spread within a population. Finally, numerical simulations are carried out, and the results are presented through illustrative figures to visually demonstrate the effectiveness of the proposed model and provide key insights into the dynamics of HPV infection.

2. Model Formation

To better understand the transmission dynamics of HPV and its progression to cervical cancer, we develop a mathematical model that captures the key stages of the infection and disease progression. The total female population is divided into six compartments, $S(t)$, Susceptible individuals, $I_{HPV}(t)$, HPV-infected individuals, $T_{HPV}(t)$ HPV-infected with treatment individuals, $T_{\widehat{HPV}}$, HPV-infected without treatment individuals, cervical cancer individuals $C(t)$ and recovered individuals $R(t)$. To depict the course of HPV illness from someone who is susceptible to HPV infection to cancer, we developed a compartmental model. In the model formulation, the dynamics of HPV transmission and its progression to cervical cancer are fundamentally described by the inflow and outflow rates established in model (1).

$$\begin{aligned}
\frac{dS}{dt} &= \Delta - \beta S I_{HPV} - \mu S + \psi R,\\
\frac{dI_{HPV}}{dt} &= \beta S I_{HPV} - (\mu+\delta) I_{HPV},\\
\frac{dT_{HPV}}{dt} &= \tau\delta I_{HPV} - (\eta+\mu) T_{HPV},\\
\frac{dT_{\widehat{HPV}}}{dt} &= (1-\tau)\delta I_{HPV} - (\alpha+\mu) T_{\widehat{HPV}},\\
\frac{dC}{dt} &= \xi\eta T_{HPV} + \alpha T_{\widehat{HPV}} - (\mu+\mu_1) C,\\
\frac{dR}{dt} &= (1-\xi)\eta T_{HPV} - (\mu+\psi) R,
\end{aligned} \tag{1}$$

with initial conditions $S(0) = S_0$, $I_{HPV}(0) = I_{HPV0}$, $T_{HPV}(0) = T_{HPV0}$, $T_{\widehat{HPV}} = T_{\widehat{HPV}_0}$, $C(0) = C_0$, $R(0) = R_0$. Figure 1 illustrates this compartmental model, the inflow to the susceptible compartment $S(t)$ is characterized by the recruitment rate Δ, while outflows occur due to the transition into HPV-infected status at a rate governed by the transmission parameter β, hence represented by the term $\beta S I_{\text{HPV}}$. The infected individuals $I_{\text{HPV}}(t)$ can transition to treatment compartments $T_{\text{HPV}}(t)$ and $\hat{T}_{\text{HPV}}(t)$, with the efficacy of these treatments represented by the parameter τ. Both treated and untreated individuals exhibit outflows, with treated individuals recovering at a rate η and untreated individuals potentially progressing to cervical cancer at a rate δ. The progression to cervical cancer is further compounded by a parameter α that describes the transition from untreated HPV cases to cervical cancer cases $C(t)$. Moreover, recovered individuals $R(t)$ experience a loss of immunity, represented by the rate ψ, which allows for their return to the susceptible population $S(t)$. Table 1 also includes all of the parameter descriptions.

The model is instrumental in analyzing the interplay of treatment efficacy and natural mortality on disease progression. By examining how alterations in these parameters impact overall health outcomes, this framework becomes essential for guiding

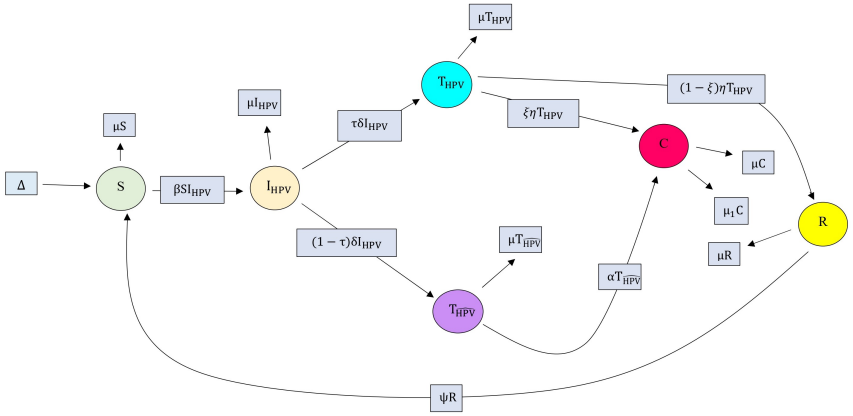

Figure 1. Diagrammatic structure for the HPV transmission dynamics.

Table 1. Description of Parameters Used in the Model

Parameter	Description
Δ	Recruitment rate
β	Disease transmission rate
μ	Natural mortality rate
ψ	Rate of loss of immunity
δ	Outflow rate from infected class
τ	Proportion of infected individuals receiving treatment
η	Outflow rate from infected individuals with treatment class
α	Progression rate to cervical cancer (without treatment)
μ_1	Mortality rate of individuals with cervical cancer
ξ	Proportion of individuals progressing to cervical cancer

public health interventions. The quantitative approach encapsulated in this model not only forecasts HPV transmission and cervical cancer incidence but also informs the development of effective vaccination and screening strategies, ultimately contributing to ongoing efforts to mitigate the global burden of cervical cancer. The model incorporates parameters that govern these transitions, allowing for an analysis of factors such as treatment efficacy and natural mortality that influence disease progression. Moreover, Figure 1 permits the examination of how changes in these parameters affect overall outcomes, which is essential for informing public health interventions. By providing a quantitative approach to forecasting HPV transmission and cervical cancer incidence, this model aids in developing effective vaccination and screening strategies, ultimately contributing to efforts aimed at reducing the global burden of cervical cancer.

3. Fundamental properties and analysis

3.1. Positivity of solution

Since the dynamics of the human population are described by model (1), all state variables and related parameters must be non-negative for any given time $t \geq 0$. This guarantees that the model solutions have biological significance because it is unrealistic to have negative population values. This finding establishes that the solutions for the state variables are not negative.

Theorem 1. *Consider the non-negative initial conditions* $\Big\{(S(0), I_{HPV}(0), T_{HPV}(0), T_{\widehat{HPV}}(0), C(0), R(0)) \in \mathbb{R}^6_+\Big\}$. *Then, the solution set* $(S(t), I_{HPV}(t), T_{HPV}(t), T_{\widehat{HPV}}(t), C(t), R(t))$ *of the model (1), remains non-negative for all* $t > 0$.

Proof. By first equation,

$$\frac{dS}{dt} = \Delta - \beta S I_{HPV} - \mu S + \psi R,$$
$$\frac{dS}{dt} \geq -(\beta I_{HPV} + \mu)S,$$
$$S(t) \geq C_1 e^{-(\beta I_{HPV}+\mu)t}.$$

By applying initial condition $t = 0, S(0) \geq C_1$ then

$$S(t) \geq S(0)e^{-(\beta I_{HPV}+\mu)t} \geq 0 \text{ since}, (\beta I_{HPV} + \mu) > 0$$

. Similar results may be obtained for $S(t) > 0$, $I_{HPV}(t) > 0$,$T_{HPV}(t) > 0$, $T_{\widehat{HPV}}(t) > 0$, $C(t) > 0$, $R(t) > 0$. Thus, for any non-negative initial conditions, all solutions model (1) stay positive. □

3.2. Invariance Property

For the purposes of epidemiology, it is essential that model (1) guarantees that the solutions stay within a biologically bounded region for all time t. This implies that the total population and all state variables are uniformly bounded, preventing unrealistic growth of the system. Under appropriate initial conditions, the solutions of model (1) remain confined within a compact positively invariant region, which ensures the epidemiological relevance and mathematical well-posedness of the model.

Theorem 2. *The region*

$$D : \Big\{(S(t), I_{HPV}(t), T_{HPV}(t), T_{\widehat{HPV}}(t), C(t), R(t)) \in \mathbb{R}^6_+ : 0 < N \leq \frac{\Delta}{\mu}\Big\},$$

is positively-invariant and attracts all the solution in $\mathbb{R}^6_+$.

Proof. In the model (1), the total population equation is obtained by adding all the compartmental equations together.

$$\begin{aligned} \frac{dN}{dt} &= \Delta - N\mu - \mu_1 C, \\ \frac{dN}{dt} &\leq \Delta - N\mu, \\ \frac{dN}{dt} + N\mu &\leq \Delta. \end{aligned} \tag{2}$$

Solving the eq. (2), $N \leq \frac{\Delta}{\mu} + (N_0 + \frac{\Delta}{\mu})e^{-\mu t}$. We get $0 \leq N \leq \frac{\delta}{\mu}$ as $t \to \infty$ by applying the theorem provided by [22] to the differential inequality previously mentioned. Since no solution path exits through the region D's boundary, under the flow represented by model (1), the region D is a positively-invariant set. It is sufficient to take the dynamics of region D in the model (1) into account. □

4. Existence of equilibrium

We examine the existence of equilibrium points, where the system reaches a steady state and all derivatives equal zero, in order to assess the model (1) long-term behavior. Two biologically significant equilibrium points are admitted by the model: the endemic equilibrium (EE) and the disease-free equilibrium (DFE).

- The disease-free equilibrium: The steady state, a point when there is absence of illness $I^*_{HPV} = T^*_{HPV} = T^*_{\widehat{HPV}} = C^* = R^* = 0$. The term disease-free equilibrium (DFE) is provided by:

$$\begin{aligned} E^* &= (S^*, I^*_{HPV}, T^*_{HPV}, T^*_{\widehat{HPV}}, C^*, R^*), \\ &= \left(\frac{\Delta}{\mu}, 0, 0, 0, 0, 0\right) \end{aligned}$$

- The endemic equilibrium: The steady state where there is infection (presence of infection) a point where $I^{**}_{HPV} \neq 0$ is called endemic equilibrium (EE) which is given by:

$$\begin{aligned} E^{**} &= (S^{**}, I^{**}_{HPV}, T^{**}_{HPV}, T^{**}_{\widehat{HPV}}, C^{**}, R^{**}), \\ S^{**} &= \frac{(\mu+\delta)}{\beta}, \\ I^{**}_{HPV} &= \frac{(\eta+\mu)T^{**}_{HPV}}{\tau\delta}, \\ T^{**}_{HPV} &= \frac{(\Delta\beta - \mu(\mu+\delta))(\mu+\psi)\tau\delta}{\beta((\mu+\delta)(\eta+\mu)(\mu+\psi) - \tau\delta\psi(1-\xi)\eta)}, \\ T^{**}_{\widehat{HPV}} &= \frac{(1-\tau)\delta(\eta+\mu)T^{**}_{HPV}}{\tau\delta(\alpha+\mu)}, \\ C^{**} &= \frac{(\xi\eta\tau\delta(\alpha+\mu) + \alpha(1-\tau)\delta(\eta+\mu))T^{**}_{HPV}}{\tau\delta(\alpha+\mu)(\mu+\mu_1)}, \\ R^{**} &= \frac{(1-\xi)\eta T^{**}_{HPV}}{(\mu+\psi)}. \end{aligned}$$

5. Basic reproduction number

The fundamental reproduction number, $\mathcal{R}_0$, assesses the likelihood of an illness spreading among a population. Here is the corrected and polished version: $\mathcal{R}_0$ is a threshold value that determines the stability of a disease-free equilibrium and is related to both the peak and the final size of an epidemic. It is described as the anticipated number of subsequent cases of infection that would arise as a result of a primary case in a perfectly susceptible population [23, 24]. To compute $\mathcal{R}_0$, we apply the next generation matrix method. First, we identify the infected compartments, which in this model are:

$$\mathbf{X} = \begin{pmatrix} I_{HPV} \\ T_{HPV} \\ T_{\widehat{HPV}} \end{pmatrix}.$$

The model equations can be written in the form:

$$\frac{d\mathbf{X}}{dt} = \mathcal{F}(\mathbf{X}) - \mathcal{V}(\mathbf{X}),$$

where:

- $\mathcal{F}(\mathbf{X})$ represents the rate of new infections,
- $\mathcal{V}(\mathbf{X})$ represents the rate of transfer between compartments (excluding new infections).

$$\begin{aligned} F &= \begin{pmatrix} \beta S I_{HPV} \\ 0 \\ 0 \end{pmatrix}, \\ V &= \begin{pmatrix} (\mu+\delta)I_{HPV} \\ -\tau\delta I_{HPV} + (\eta+\mu)T_{HPV} \\ (\alpha+\mu)T_{\widehat{HPV}} - (1-\tau)\delta I_{HPV} \end{pmatrix}, \\ \mathfrak{F} &= \begin{pmatrix} \frac{\beta\Delta}{\mu} & 0 & 0 \\ 0 & 0 & 0 \\ 0 & 0 & 0 \end{pmatrix}, \\ \mathfrak{V} &= \begin{pmatrix} \mu+\delta & 0 & 0 \\ -\tau\delta & \eta+\mu & 0 \\ -(1-\tau)\delta & 0 & \alpha+\mu \end{pmatrix}, \\ \mathfrak{F}\mathfrak{V}^{-1} &= \begin{pmatrix} \frac{\beta\Delta}{\mu(\mu+\delta)} & 0 & 0 \\ 0 & 0 & 0 \\ 0 & 0 & 0 \end{pmatrix}. \end{aligned}$$

Then,

$$\mathcal{R}_0 = \frac{\beta\Delta}{\mu(\mu+\delta)}.$$

Understanding $\mathcal{R}_0$ is critical, as values greater than 1 indicate that the disease is likely to spread, while values less than 1 suggest eventual decline and possible eradication. Accurate estimation of$\mathcal{R}_0$allows public health officials to gauge the potential for outbreaks and develop effective strategies for intervention and control, underscoring its role in disease management planning. Moreover, it is essential to distinguish $\mathcal{R}_0$ from the effective reproduction number $\mathcal{R}$, which accounts for changes in population immunity and behavior due to interventions like vaccination and social distancing, making $\mathcal{R}_0$ a vital metric in assessing ongoing control measures.

6. Stability analysis

To understand the long-term behavior of the model, we analyze the stability of its equilibrium points. The disease-free equilibrium is analyzed first since it indicates whether the infection can invade the population. If the disease-free equilibrium becomes unstable $\mathcal{R}_0 > 1$, we further analyze the endemic equilibrium to study the persistence of the infection. We now proceed to study the local stability of the disease-free equilibrium E^*.

Theorem 3. *The E^* of model (1) is Locally Asymptotically Stable (LAS) if $\mathcal{R}_0 < 1$ and unstable if $\mathcal{R}_0 > 1$.*

Proof. The Jacobian matrix at E^* is given by

$$\mathcal{J}_{\mathcal{E}^*} = \begin{pmatrix} -\mu & \Psi_1 & 0 & 0 & 0 & \psi \\ 0 & \Psi_2 & 0 & 0 & 0 & 0 \\ 0 & \tau\delta & \Psi_3 & 0 & 0 & 0 \\ 0 & \Psi_4 & 0 & \Psi_5 & 0 & 0 \\ 0 & 0 & \xi\eta & \alpha & \Psi_6 & 0 \\ 0 & 0 & \Psi_7 & 0 & 0 & \Psi_8 \end{pmatrix},$$

$$\Psi_1 = \frac{-\beta\Delta}{\mu}, \quad \Psi_2 = \frac{\beta\Delta}{\mu} - (\mu+\delta),$$
$$\Psi_3 = -(\eta+\mu), \quad \psi_4 = (1-\tau)\delta,$$
$$\Psi_5 = -(\alpha+\mu), \quad \Psi_6 = -(\mu+\mu_1),$$
$$\Psi_7 = (1-\xi)\eta, \quad \Psi_8 = -(\mu+\psi).$$

The characteristic roots can be found as $\lambda_1 = -\mu, \lambda_2 = \mathcal{R}_0 - 1, \lambda_3 = -(\eta+\mu), \lambda_4 = -(\alpha+\mu), \lambda_5 = -(\mu+\mu_1), \lambda_6 = -(\mu+\psi)$. When $\mathcal{R}_0 < 1$, we have $\lambda_2 < 0$. In this instance, all of $\mathcal{J}_{\mathcal{E}^*}$'s roots are negative. As a result, E^* is LAS. When $\mathcal{R}_0 > 1$, we get $\lambda_2 > 0$, and $\mathcal{J}_{\mathcal{E}^*}$ have positive roots, so E^* is unstable. □

The local stability of the disease-free equilibrium point E^* is critically dependent on the value of $\mathcal{R}_0$. When $\mathcal{R}_0 < 1$, the equilibrium is locally asymptotically stable, indicating that any perturbations in the population will eventually return to the disease-free state, proving that the disease can be effectively controlled. Conversely, when $\mathcal{R}_0 > 1$, the unstable nature of E^* signifies that the disease will likely persist and spread in the population, reinforcing the need for aggressive intervention strategies to reduce transmission. Thus, the critical threshold provided by $\mathcal{R}_0$ serves as a decisive indicator of the potential for epidemic spread, guiding public health responses and resource allocation in managing infectious diseases.

7. Sensitivity analysis

Assess the robustness of $\mathcal{R}0$ by conducting a parameter contribution analysis. Any modifications or errors in the formulation or computation of $\mathcal{R}0$ can lead to changes in parameter values and underlying model assumptions. Thus sensitivity analyses are performed to pinpoint those modifications and inaccuracies additionally the effects they have on the model. The ratio of the percentage change in a variable to the change in a certain parameter is known as the normalised forward sensitivity index (NFSI) of that variable as regards of that parameter. Check out [25] for more details. Below, the NFSI with relation to each of the parameters is calculated to examine the sensitivity of $\mathcal{R}_0$ regarding each of its aspects.

From the sensitivity analysis, a positive sensitivity index indicates that decrease(increase) value of the parameter results in decrease(increase) in $\mathcal{R}_0$, whereas negative sensitivity index results in decrease(increase) value of the parameter to increase(decrease) in $\mathcal{R}_0$.

$$\Lambda_x^{\mathcal{R}_0} = \frac{\partial\mathcal{R}_0}{\partial x} \times \frac{x}{\mathcal{R}_0}$$

for every basic parameter is represented by x and

$$\mathcal{R}_0 = \frac{\beta\Delta}{\mu(\mu+\delta)},$$

then,

$$\Lambda_\beta^{\mathcal{R}_0} = \frac{\partial\mathcal{R}_0}{\partial\beta} \times \frac{\beta}{\mathcal{R}_0} = 1$$
$$\Lambda_\Delta^{\mathcal{R}_0} = \frac{\partial\mathcal{R}_0}{\partial\Delta} \times \frac{\Delta}{\mathcal{R}_0} = 1$$
$$\Lambda_\delta^{\mathcal{R}_0} = \frac{\partial\mathcal{R}_0}{\partial\delta} \times \frac{\delta}{\mathcal{R}_0} = -\frac{\delta}{(\mu+\delta)}$$
$$\Lambda_\mu^{\mathcal{R}_0} = \frac{\partial\mathcal{R}_0}{\partial\mu} \times \frac{\mu}{\mathcal{R}_0} = -\frac{2\mu+\delta}{(\mu+\delta)}$$

8. Numerical Analysis

The simulation will use the parameters listed in Tables 2 and 3, with all parameter values expressed on a per-day basis. The literature and presumptions were used to get the values for the parameters. These simulations aim to highlight some of the theoretical findings made in this research. The parameters applied to Case I are in Table 2, given initial conditions $S_0 = 100, I_{HPV0} = 50, T_{HPV0} = 30, T_{\widehat{HPV}_0} = 20, C_0 = 10, R_0 = 0$. The illustrations for Case I are expressed in Figures 4a, 5b and 8a. In instance II, some of the parameters are randomly selected and some are obtained from the literature (Table 3). The appropriate simulation are displayed in Figure 6a through Figures 7b and 8b. These graphs aid in the comprehension of disease transmission.

Table 2. Case I

Parameter	Value
Δ	10
β	0.8
μ	0.0576
ψ	0.35
δ	0.314
τ	0.85
η	0.23
α	0.1217
μ_1	0.12745
ξ	0.35

Table 2 for Case I, is a set of carefully selected parameters is employed to comprehensively study the dynamics of HPV transmission and its progression to cervical cancer. The parameter Δ is assumed to be 10, reflecting the entry rate of new susceptible individuals into the population. The transmission rate β is set at 0.8, which, indicates a high potential for disease spread, while the natural mortality rate μ is established at 0.0576 to represent the baseline mortality within the population. The recovery rate ψ is assumed to be 0.35, demonstrating the proportion of infected individuals recovering over time, and the disease progression rate δ is set at 0.314, highlighting the transition rate of infected individuals to cervical cancer. Additionally, the treatment rate τ is defined as 0.85, suggesting a substantial effectiveness of treatment in reducing transmission, whereas the progression to

cancer rate η is assumed to be 0.23, underscoring the risks associated with untreated infections. The recovery rate of treated individuals α is noted as 0.1217, indicating the effectiveness of therapeutic interventions, alongside a secondary mortality rate μ_1 of 0.12745, reflecting the mortality risk for those with cervical cancer. Finally, the miscellaneous transition parameter ξ is assumed to be 0.35, capturing additional transitions within the model that may influence disease dynamics. Collectively, these parameters are critical for assessing the interaction between various health states, ultimately aiming to inform public health strategies and interventions to combat HPV-related health issues effectively.

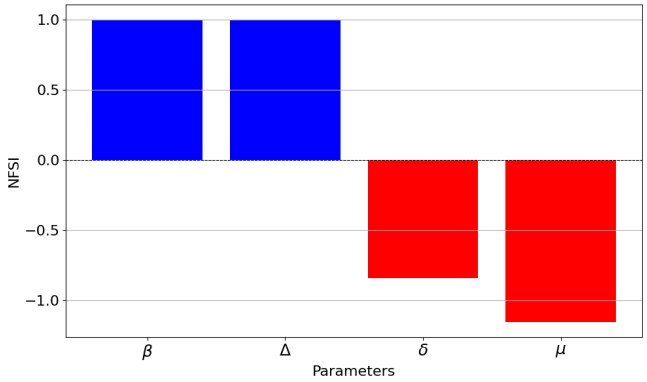

Figure 2. Normalized Forward Sensitivity Index (NFSI) of the basic reproduction number ($\mathcal{R}_0$).

The critical relationships between the basic reproduction number $\mathcal{R}_0$ and its parameters are examined. The positive sensitivity indices for $\Lambda_\beta^{\mathcal{R}_0}$ and $\Lambda_\Delta^{\mathcal{R}_0}$ suggest that increases in the transmission rate β and the recruitment rate Δ directly enhance $\mathcal{R}_0$, thereby indicating that these factors are pivotal for disease spread. In contrast, the negative sensitivity indices for both $\Lambda_\delta^{\mathcal{R}_0}$ and $\Lambda_\mu^{\mathcal{R}_0}$ indicate that increasing disease progression rates δ and natural mortality rates μ would reduce$\mathcal{R}_0$. This highlights the potential for intervention strategies focused on reducing these parameters to effectively lower $\mathcal{R}_0$ and control disease transmission.

The Figure 2 displays the Normalized Forward Sensitivity Index (NFSI) of the basic reproduction number ($\mathcal{R}_0$) for key parameters in an HPV infection model. Positive NFSIs (β, Δ) indicate that increasing these parameters raises $\mathcal{R}_0$, while negative NFSIs (δ, μ) show that increasing them lowers $\mathcal{R}_0$. This reveals which parameters most strongly influence disease spread, informing targeted interventions. The findings highlight the crucial roles of transmission rate and recruitment in driving $\mathcal{R}_0$ and the mitigating effects of progression and death rates.

Figure 3 visualizes the sensitivity of the basic reproduction number ($\mathcal{R}_0$). Positive indices for transmission (β) and recruitment (Δ) rates signify that increasing these parameters increases $\mathcal{R}_0$, while negative indices for disease progression (δ) and natural mortality (μ) rates indicate that increasing them decreases $\mathcal{R}_0$. This highlights parameters most influential on disease spread, guiding intervention strategies.

The Figures 4a and 4b present simulations of HPV infection dynamics, offering insights into the progression and management of the disease. Figure 4a simulates the dynamics of HPV infections over time, providing a detailed understanding of

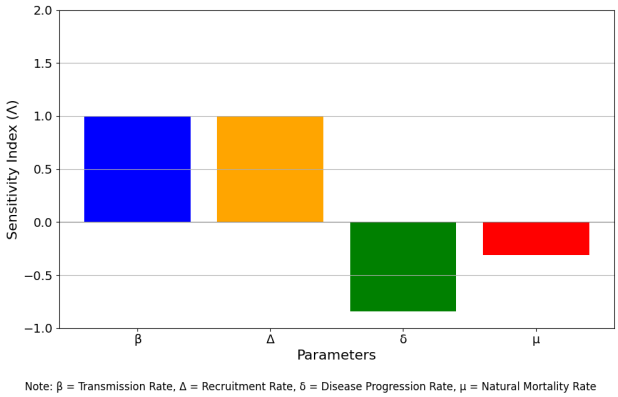

Figure 3. Sensitivity Analysis of Basic Reproduction Number ($\mathcal{R}_0$).

the natural progression of the disease. The simulation is based on key parameters, including $\Delta = 10$, $\beta = 0.8$, $\mu = 0.0576$, $\psi = 0.35$, $\delta = 0.314$, $\tau = 0.85$, $\eta = 0.23$, $\alpha = 0.1217$, and $\mu_1 = 0.12745$. The graph illustrates a sharp initial rise in the number of infected individuals, reflecting the rapid early spread of the infection, followed by a gradual decline, suggesting that HPV infection rates may self-regulate over time in the absence of intervention. The horizontal axis represents time, while the vertical axis shows the number of infected individuals, highlighting the temporal trend of HPV infections. This simulation offers valuable insights into the dynamics of HPV transmission, the potential for infection stabilization, and the progression within a population, making it a critical tool for informing public health strategies. Whereas, Figure 4b illustrates the dynamics of HPV infections when a treatment intervention is introduced at a specific point in time. The simulation is based on same key parameters, including and tracks the number of infected individuals over time. The graph reveals a noticeable decrease in infections following the application of treatment, underscoring its effectiveness in managing HPV. This decline highlights the potential impact of timely and targeted treatment strategies in controlling the spread of the virus within the population. By demonstrating the influence of interventions, the simulation provides valuable insights for evaluating and optimizing treatment approaches to combat HPV infections. These findings emphasize the critical role of treatment in reducing infection rates and support the development of evidence-based public health strategies to manage the disease effectively.

The Figures 5a and 5b provide a detailed comparison of HPV infection dynamics in two distinct scenarios. Figure 5a illustrates the dynamics of HPV infections in the absence of treatment, offering valuable insights into the natural progression of the disease. The simulation tracks the number of infected individuals over time, revealing a steady increase in infections as the virus spreads unchecked. This trend emphasizes the persistent and escalating nature of HPV infections when no intervention is applied. By providing a baseline scenario, the figure highlights the stark contrast between untreated progression and potential outcomes with effective treatment strategies. Also the Figure 5b presents a graph that compares the survival probabilities over time between treated and untreated cervical cancer patients. It demonstrates that patients who receive treatment

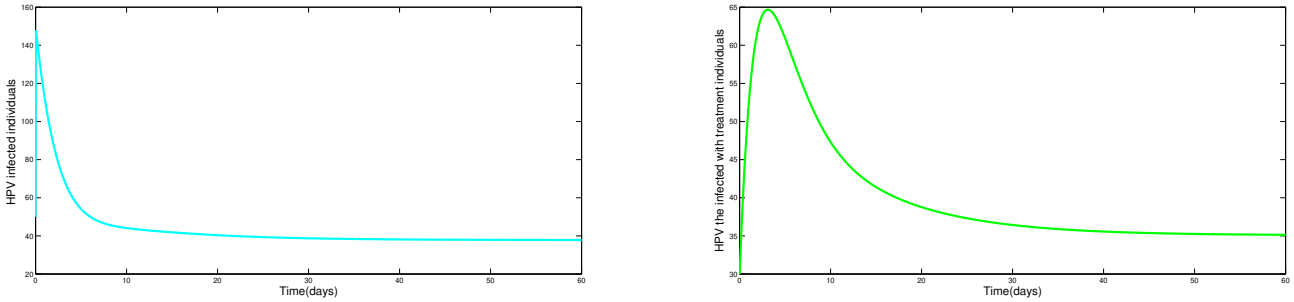

(a) (b)

Figure 4. (a) Simulation of HPV infected individuals. (b) Simulation of HPV the infected with treatment individuals.

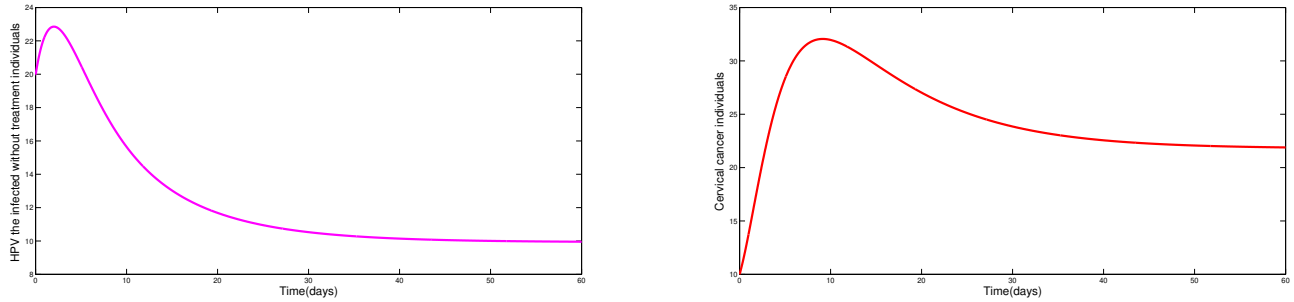

(a) (b)

Figure 5. (a) Simulation of HPV the infected without treatment individuals. (b) Simulation of cervical cancer individuals.

have significantly higher survival rates compared to those who do not. This finding suggests that effective treatment interventions can greatly improve prognosis for cervical cancer.This insight can inform clinical decision-making and guide the development of more impactful cervical cancer management strategies. The simulation provides quantitative evidence of the potential benefits of treatment in enhancing patient outcomes. The parameters defined in Table 3 for Case II provide a refined perspective on the dynamics of HPV infection and its potential progression to cervical cancer. Employing the same baseline value for Δ at 10, we aim to investigate how varying other parameters influences disease transmission and recovery outcomes. The transmission rate β remains constant at 0.8, indicating that the disease retains the high contagion potential characterized in Case I. However, significant changes are observed in the recovery-related parameters, reflective of an altered treatment scenario. In this case, the recovery rate ψ is substantially lower at 0.00035, suggesting a much lower efficiency of treatment or a focus on individuals who are more severely affected. This change could imply that the population modeled in Case II has less access to effective healthcare or that the treatments currently available are not as effective as previously thought. The progression rate δ is increased to 0.514, indicating that individuals transition to a state of cervical cancer more rapidly than in Case I. This is a critical change that emphasizes the potential urgency for interventions and may point to more severe disease pathology or a higher prevalence of high-risk HPV strains in this scenario. The treatment rate τ remains consistent at 0.85, affirming the importance of treatment in this model, yet the implications of the lowered recovery rate suggest that even with established treatments, their effectiveness may be compromised in the cohort represented in Case II. Additionally, for recovery rates from treatment α, the value is lower at 0.01217, further reinforcing the suggestion that effective recovery from HPV infections is less likely in this modeled population. The mortality associated with cervical cancer defined by μ_1 remains unchanged at 0.12745, aligning with literature values, yet the impact of the other adjustments will be critical in understanding the broader implications on public health outcomes. The new miscellaneous transition parameter ξ is also set at 0.00035, indicating the potential for additional factors influencing recovery that were not accounted for previously. The simulations derived from these parameters are depicted in Figure 6a to Figure 8b. Notably, the outcome visualizations will allow us to compare trends in HPV infection rates, the effects of

Table 3. Case II

Parameters	Values
Δ	10
β	0.8
μ	0.0576
ψ	0.00035
δ	0.514
τ	0.85
η	0.23
α	0.01217
μ_1	0.12745
ξ	0.00035

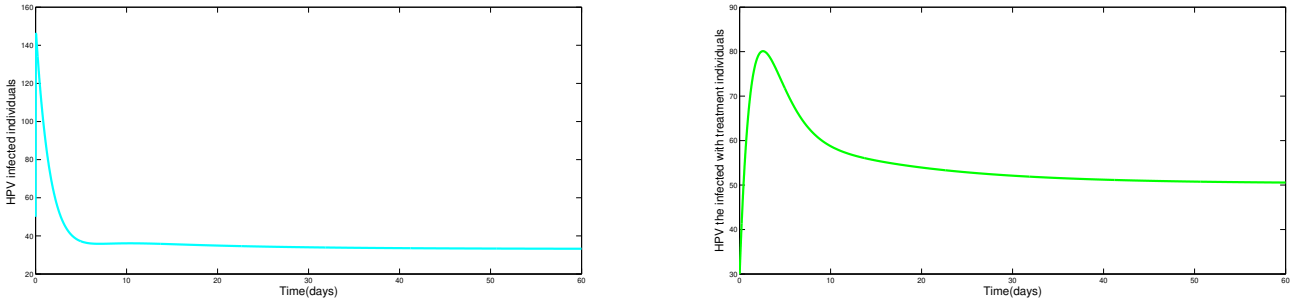

(a) (b)

Figure 6. (a) Simulation of HPV infected individuals. (b) Simulation of HPV the infected with treatment individuals.

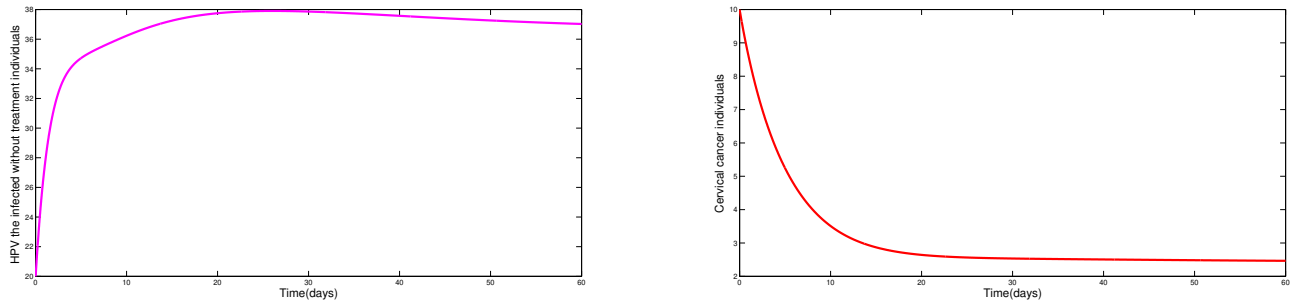

(a) (b)

Figure 7. (a) Simulation of HPV the infected without treatment individuals. (b) Simulation of cervical cancer individuals.

treatment, and the progression to cervical cancer within the different parameter frameworks established by Case I and Case II. In essence, the modifications in Case II's parameters construct a narrative illustrating the complexities of HPV infection dynamics. They underscore how changes in treatment efficacy and disease progression rates can heavily influence health outcomes and highlight the critical need for enhanced healthcare strategies to manage these infections effectively.

The Figures 6a and 6b provide a detailed comparison of HPV infection dynamics in recurrent cancer rates for individuals with HPV-related cancer and the simulation of HPV infection with treatment. The Figure 6a presents a simulation of recurrent cancer rates for individuals with HPV-related cancer, illustrating the probability of cancer recurrence over time and comparing treated versus untreated individuals. The graph demonstrates that the recurrence rate is notably lower for those who undergo treatment, emphasizing the potential of treatment in reducing the likelihood of cancer relapse. These findings highlight the significant role that treatment can play in preventing recurrence, which is critical for improving long-term outcomes and managing HPV-related cancer effectively. By examining these probabilities of recurrence, the simulation underscores the importance of timely and targeted interventions to prevent cancer relapse and improve the prognosis of affected individuals. In Figure 6b, a simulation of HPV infection with treatment is presented, confirming the findings of Figures 4a and 5a by showing the significant reduction in infection rates after the introduction of treatment. The graph tracks the number of infected individuals over time, demonstrating the effectiveness of the treatment in controlling HPV infections. This consistency across multiple simulations highlights the potential of targeted treatment strategies to effectively manage HPV infection and reduce its spread.

The Figures 7a and 7b provide a detailed comparison of HPV infection dynamics in Simulation of HPV the infected without treatment individuals and cervical cancer individuals. Figure 7a simulates the natural progression of HPV infections over time without any treatment intervention. The graph shows a steady increase in the number of infected individuals, indicating that HPV can spread rapidly in a population in the absence of effective management strategies. This baseline scenario underscores the critical importance of implementing appropriate treatment and prevention measures to control the spread of HPV. Whereas, Figure 7b simulates the impact of treatment on HPV-infected individuals. The graph demonstrates a decrease in infections after the introduction of a treatment intervention. This finding suggests that effective treatment approaches can significantly reduce the prevalence of HPV in a population. The simulation provides quantitative evidence of the potential benefits of treatment in managing the spread of HPV.

Figures 8a and 8b depitcs the simulation of HPV Recovered individulas od Case 1 and Case 2, the Figure 8a explains the survival probability over time for cervical cancer patients who do not receive treatment. The graph shows a lower survival rate for untreated individuals, indicating a poorer prognosis for cervical cancer without appropriate interventions. This insight can inform clinical decision-making and the development of more ef-

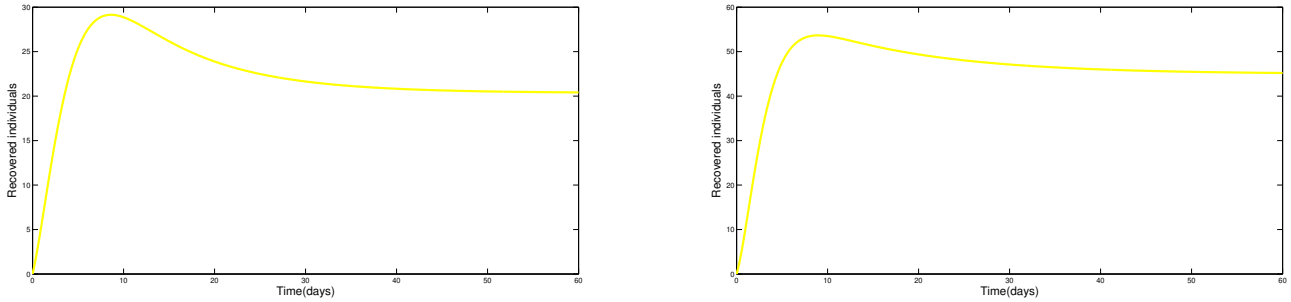

(a) (b)

Figure 8. (a) Simulation of recovered individuals parametric values from case I. (b) Simulation of recovered individuals parametric values from case II.

fective cervical cancer management strategies, and in Figure 8b simulates the progression of cervical cancer in individuals who undergo treatment. The graph illustrates higher survival probabilities for treated patients compared to the untreated scenario shown in Figure 8a. This finding suggests that effective treatment interventions can greatly improve the long-term outcomes for cervical cancer patients. The simulation provides quantitative evidence of the potential benefits of treatment in enhancing patient survival.

9. Conclusion

Cervical cancer remains a significant global health challenge, particularly in low- and middle-income countries, where it ranks among the most prevalent malignancies affecting women. This study developed a deterministic compartmental mathematical model to quantitatively analyze the dynamics of HPV transmission and its progression to cervical cancer. By examining the reproduction number ($\mathcal{R}_0$) and the associated disease-free and endemic equilibria, we gained critical insights into the factors driving disease dynamics. Sensitivity analysis identified key parameters influencing $\mathcal{R}_0$, providing valuable directions for targeted interventions. In the future, these models can be explored in greater depth using real-world datasets to validate findings and enhance applicability. Additionally, expanding the framework to incorporate other compartments and leveraging fractional differential equations could provide a deeper understanding of disease dynamics. The outcomes of this research contribute to the growing body of knowledge needed to inform effective strategies for controlling HPV transmission and mitigating cervical cancer incidence.

Author Contributions. **Jose, S. A.**: Conceptualization, Data curation, Formal analysis, Investigation, Methodology, Resources, Software, Validation, visualization, Writing – original draft, Writing – review & editing. **Nelson, S. P.**: Formal analysis, Investigation, Methodology, Resources, Validation, visualization, Writing – review & editing. **Raja, R.**: Formal analysis, Investigation, Methodology, Resources, Validation, Supervision, Writing – review & editing. **Menon. G. R.**: Formal analysis, Investigation, Methodology, Resources, Validation, visualization, Writing – review & editing. **Jirawattanapanit, A.**: Formal analysis, Investigation, Methodology, Project administration, Software, Supervision, Validation, Visualization, Writing – review & editing.

Acknowledgement. The researcher acknowledges the valuable support provided by the Research and Development Institute and the substantial institutional support from Phuket Rajabhat University.

Funding. This research received no external funding.

Conflict of interest. The authors declare no conflict of interest.

Data availability. Not applicable.

References

[1] R. Thomas *et al.*, "Modeling and analysis of SEIRS epidemic models using homotopy perturbation method: a special outlook to 2019-nCoV in India," *International Journal of Biomathematics*, vol. 15, no. 8, p. 2250059, 2022. DOI:10.1142/S1793524522500590

[2] S. A. Jose *et al.*, "An integrated eco-epidemiological plant pest natural enemy model with different impulsive strategies," *Mathematical Problems in Engineering*, vol. 2022, no. 1, p. 4780680, 2022. DOI:10.1155/2022/4780680.

[3] S. A. Jose *et al.*, "Impact of strong determination and awareness on substance addictions: a mathematical modeling approach," *Mathematical Methods in the Applied Sciences*, vol. 45, no. 8, pp. 4140–4160, 2022. DOI:10.1002/mma.7859

[4] S. A. Jose *et al.*, "Mathematical modeling on transmission and optimal control strategies of corruption dynamics," *Nonlinear Dynamics*, vol. 109, no. 4, pp. 3169–3187, 2022. DOI:10.1007/s11071-022-07581-6

[5] S. A. Jose *et al.*, "Stability analysis and comparative study on different ecoepidemiological models: stage structure for prey and predator concerning impulsive control," *Optimal Control, Applications and Methods*, vol. 43, no. 3, pp. 842–866, 2022. DOI:10.1002/oca.2856

[6] M. Arunkumar, P. K. Rajan, and K. Murugesan, "Mathematical analysis of an optimal control problem for mitigating hpv transmission and cervical cancer progression through educational campaigns," *Iranian Journal of Science*, vol. 49, pp. 1309–1325, 2025. DOI:10.1007/s40995-025-01804-2

[7] S. P. Nelson *et al.*, "Modeling the dynamics of COVID-19 in Japan: employing data-driven deep learning approach," *International Journal of Machine Learning and Cybernetics*, vol. 16, pp. 7045–7958, 2025. DOI:10.1007/s13042-024-02301-5

[8] WHO, "Cervical cancer is the fourth most common cancer in women, with around 660,000 cases and 350,000 deaths globally in 2022," https://www.who.int/news-room/fact-sheets/detail/cervical-cancer, 2022, Accessed on 6 January 2025.

[9] ACS, "Cervical Cancer Risk Factors," https://www.cancer.org/cancer/cervical-cancer/causes-risks-prevention/risk-factors.html, 2022, Accessed on 6 January 2025.

[10] NIC, "Cervical Cancer Prevention and Risk Factors," https://www.cancer.gov/types/cervical/causes-risk-prevention, 2024, Accessed on 6 January 2025.

[11] CDC, "Genital HPV Infection: CDC Fact Sheet," https://www.cdc.gov/sti/about/about-genital-hpv-infection.html, 2025, Accessed on 6 January 2025.

[12] A. S. Bergot *et al.*, "New approaches to immunotherapy for HPV associated cancers," *Cancers*, vol. 3, no. 3, pp. 3461–3495, 2011. DOI:10.3390/cancers3033461

[13] U.S. Census Bureau, "American Community Survey," *U.S. Census Bureau*, 2010, Accessed on 6 January 2025.

[14] J. M. Crow, "HPV: the global burden," *Nature*, vol. 488, no. 7413, pp. S2–S3, 2012. DOI:10.1038/488S2a.

[15] D. R. Lowy and J. T. Schiller, "Prophylactic human papillomavirus vaccines," *The Journal of Clinical Investigation*, vol. 116, no. 5, pp. 1167–1173, 2006. DOI:10.1172/JCI28607

[16] J. M. Walboomers *et al.*, "Human papillomavirus is a necessary cause of invasive cervical cancer worldwide," *The Journal of Pathology*, vol. 189, no. 1, pp. 12–19, 1999. DOI:10.1002/(SICI)1096-9896(199909)189:1<12::AID-PATH431>3.0.CO;2-F

[17] Y. H. Choi *et al.*, "Transmission dynamic modelling of the impact of human papillomavirus vaccination in the United Kingdom," *Vaccine*, vol. 28, no. 24, pp. 4091–4102, 2010. DOI:10.1016/j.vaccine.2009.09.125

[18] E. J. Domingo *et al.*, "Epidemiology and prevention of cervical cancer in Indonesia, Malaysia, the Philippines, Thailand and Vietnam," *Vaccine*, vol. 26, suppl. 12, pp. M71–M79, 2008. DOI:10.1016/j.vaccine.2008.05.039

[19] GBD, "Global estimates of incidence and mortality of cervical cancer in 2020: a baseline analysis of the WHO Global Cervical Cancer Elimination Initiative," *The Lancet Global Health*, vol. 11, no. 2, pp. e197–e206, 2023. DOI:10.1016/S2214-109X(22)00501-0

[20] PAHO, "A Global Strategy for Elimination of Cervical Cancer," https://www.paho.org/en/end-cervical-cancer, 2020, Accessed on 6 January 2025.

[21] ACS, "Prevention of Cervical Cancer," https://www.cancer.org/cancer/cervical-cancer/prevention-and-early-detection.html, 2024, Accessed on 6 January 2025.

[22] G. Birkhoff and G. C. Rota, "*Ordinary Differential Equations*." Boston: Ginn, 1982.

[23] O. Diekmann and J. A. P. Heesterbeek, "*Mathematical Epidemiology of Infectious Diseases: Model Building, Analysis and Interpretation*." Chichester: John Wiley & Sons, 2000.

[24] W. Atkinson, S. Wolfe, and J. Hamborsky, "*Epidemiology and Prevention of Vaccine-Preventable Diseases (12th ed.)*." Washington, DC: Public Health Foundation, 2012.

[25] N. Chitnis, J. M. Hyman, and J. M. Cushing, "Determining important parameters in the spread of malaria through the sensitivity analysis of a mathematical model," *Bulletin of Mathematical Biology*, vol. 70, no. 5, pp. 1272–1296, 2008. DOI:10.1007/s11538-008-9299-0.